PERGAMON

International Journal of Multiphase Flow 25 (1999) 187–200

International Journal of Multiphase Flow

Direct numerical simulation of particle-turbulence interaction

C. Li, A. Mosyak, G. Hetsroni *

Department of Mechanical Engineering, Technion, Israel Institute of Technology, Haifa, 32000, Israel

Received 25 August 1995; received in revised form 10 July 1998

Abstract

This paper presents the results of a numerical simulation of the interaction between solid particles and near-wall turbulence. The fluid flow in a horizontal channel is solved using direct numerical simulation. For the particle motion, a Lagrangian approach is used. The particles are relatively large, and cover several collocation points in the fluid. Two-way coupling is used to account for the effect of the particles on the structure of the near-wall turbulence, and on the main stream.

It is shown that the presence of large particles in the near-wall region enhances the intensity of the carrier phase velocity fluctuations. Based on the computational data, it was established that the particles with large relaxation time move in a random way and do not accumulate along the low velocity streaks, as smaller particles do.

Keywords: Direct numerical simulation; Solid particles; Near-wall turbulence

1. Introduction

The motion of particles in turbulent flows and the interaction between particles and the turbulence have become one of the most interesting topics in fluid mechanics.

Available experimental data show that the addition of particles may increase or decrease the turbulent kinetic energy of the carrier fluid. Buyevich and Gupalo (1965) considered a decay of isotropic turbulence in a flow with small particles and showed that the presence of small particles provides an additional decay of the turbulence.

Some experiments, e.g. Hetsroni and Sokolov (1971), Tsuji et al (1988), Parthasarathy and Faeth (1987), Levy and Lockwood (1981), showed that the presence of small particles in

* Corresponding author.

0301-9322/99/$ - see front matter
PII: S0301-9322(98)00044-5

turbulent flow reduces the turbulent intensity of the carrier fluid, and presence of large particles increases the turbulent intensity. A detailed review is given by Hetsroni (1989). Recent works, Kaftori et al. (1995a, b), Nino and Garcia (1996) have also well illustrated the particle entrainment by coherent wall structures and suggest that the nature of interaction may significantly affect the carrier fluid, especially very close to the boundary.

Gore and Crowe (1989) proposed the critical parameter d_p/L (d_p is the particle diameter, L is the integral length scale of the turbulence) that predicts whether the turbulence will be augmented or suppressed with the addition of particles. In that study, the augmentation of turbulent energy by the particles is attributed to the presence of their wakes. However, experimental work by Hardalupas et al. (1989) showed that particles without wakes (small Re_p) may also increase the turbulent energy.

Vinberg et al. (1991) showed that in anisotropic flows the addition of small particles can enhance turbulence. Recently Yarin and Hetsroni (1993) showed that the ratio diameter/turbulence scale does not generalize the experimental data for different particles sizes. They proposed a simplified theory based on the modified mixing-length theory and turbulent kinetic energy balance. For coarse particles, the level of fluctuations is determined by vortex shedding. Yarin and Hetsroni (1993) also showed that the turbulent kinetic energy depends only on $\beta C_D^{3/2}$ where C_D is the drag coefficient of the particle, and and β is an empirical constant.

There is a number of direct numerical simulation studies concerning the two-way interaction of particles with turbulence. Elghobashi and Truesdell (1993) examined the turbulence modification due to the two-way interaction between decaying turbulence and small dispersed solid particles. Their results show that the particles can increase the fluid turbulence energy.

Pedinotti et al. (1992) carried out direct numerical simulation of particle behaviour in the wall region, without the feedback effects from the particles on the fluid motion. They calculated the flow field in a flume by using a pseudo-spectral direct solution of the Navier–Stokes equations, in the same way as was done in this investigation. They assumed that the particle concentration is low enough to allow the use of one-way coupling in the calculations, i.e. the fluid moves the particles but there is no feedback from the particles on the fluid motion. In our present work we concentrated on the two-way coupling, i.e. on how the particles affected the turbulence of the fluid. McLaughlin (1994) reviewed recent research on the techniques of DNS including two-way (feedback) coupling. Some aspects of the direct numerical simulation were reviewed by Banerjee (1994). Pan and Banerjee (1996), in their direct numerical simulation, accounted for the particle effect by superimposing the Stokes solution on the continuous-flow velocity field. The numerical investigation of the effects of particles on wall turbulence indicates that the ejection–sweep cycle is affected—primarily through suppression of sweeps by the smaller particles and enhancement of sweep activity by the larger particles, Pan and Banerjee (1997).

Several mechanisms of turbulence modulation may be invoked to explain particle-coherent structure intractions. These mechanisms may be significantly influenced by both particle–particle and particle–wall interactions. To clarify the effects of such phenomena on particle–wall interactions, we will focus on turbulent flow carrying particles at an average volume fraction of $2.6{\cdot}10^{-4}$.

The present study is motivated by recent experiments (Hetsroni and Rozenblit 1994) and has the primary objective of determining how particles modulate fluctuations of the carrier fluid in

the wall region. In this connection, pseudospectral calculations, based on a computer code developed by Lam and Banerjee [1] (1988), and Lam (1989), have been used to generate the fluid velocity field in a horizontal flume. The boundary conditions on the bottom wall are no-slip and the boundary conditions at the interface are free-slip. In this study, the motion of each particle is traced by the Lagrangian method, and the effect of each particle on the fluid is fed back into the flow field.

We examine in some detail the two-way coupling and interaction between large particles ($Re_p > 1$) and the turbulence in the near wall region of the open channel turbulent flow. We use Lam and Banerjee's (1988) method of direct numerical simulation to solve the three-dimensional, time-dependent Navier–Stokes equations which include all the forces exerted by the particles on the fluid.

2. Mathematical description

The time-dependent, three-dimensional Navier–Stokes and continuity equations are solved in a rectangular domain, presented in Fig. 1. The streamwise direction is denoted by x_1, the spanwise by x_2, and the wall-normal direction by x_3, while the velocity components are u_1, u_2, u_3, correspondingly. The flow is driven by a constant streamwise pressure gradient. Periodic boundary conditions are imposed in x_1 and x_2 directions. All the quantities are normalized with the effective shear velocity and the half-depth of the channel. The effective shear velocity is defined as $u^* = \sqrt{h\Pi}$, where $\Pi = (1/\rho)\partial p/\partial x_i$ is the mean kinematic pressure gradient, and h is the half-depth of the channel. The effective Reynolds number is defined as $Re = (u^* h/\nu)$, where ν is the fluid viscosity. The velocity and length are scaled by u^* and h, respectively. The non-dimensional continuity and Navier–Stokes equations for an incompressible Newtonian fluid are:

$$\frac{\partial u_i}{\partial x_i} = 0, \tag{1}$$

$$\frac{\partial u_i}{\partial t} = S_i + \frac{1}{Re}\nabla^2 u_i - \frac{\partial p}{\partial x_i} \tag{2}$$

where $\partial p/\partial x_i$ is the pressure gradient minus the mean value of the pressure gradient, and S_i are the nonlinear convective terms minus the mean kinematic pressure gradient

$$S_1 = -\frac{\partial u_1 u_i}{\partial x_j} + 1; \quad S_2 = -\frac{\partial u_2 u_j}{\partial x_j}; \quad S_3 = -\frac{\partial u_3 u_j}{\partial x_j}. \tag{3}$$

The pressure gradient $\partial p/\partial x_i$ is eliminated from the equations by taking the curl of Eq. (2) to give

[1] We gratefully acknowledge the help of professor S. Banerjee in providing us with this code.

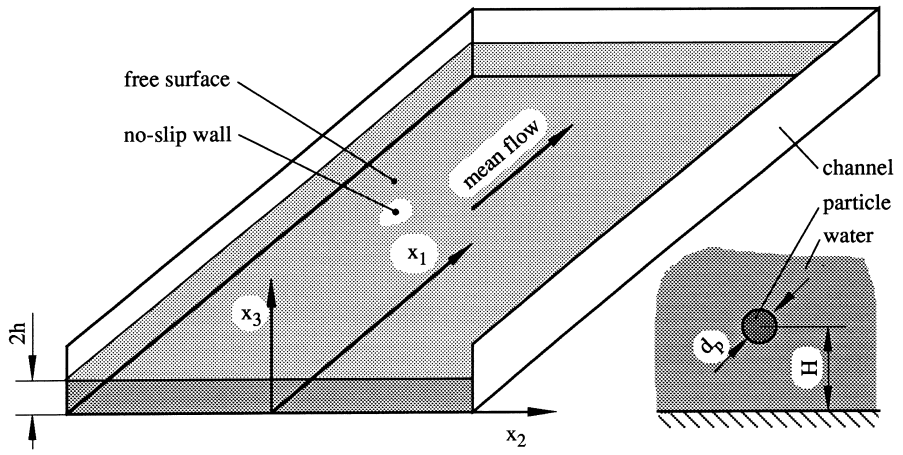

Fig. 1. Flow geometry for DNS

$$\frac{\partial \omega_k}{\partial t} = \epsilon_{ijk} \frac{\partial S_j}{\partial x_i} + \frac{1}{Re} \nabla^2 \omega_k \tag{4}$$

where ω_k is the vorticity. Taking the curl of Eq. (4) again, one obtains a fourth order equation

$$\frac{\partial}{\partial t}(\nabla^2 u_i) = \nabla^2 S_i - \frac{\partial}{\partial x_i}\left(\frac{\partial S_j}{\partial x_j}\right) + \frac{1}{Re} \nabla^4 u_i. \tag{5}$$

Eqs. (4) and (5), for the normal component, i.e. for ω_3 and u_3, are solved first. With u_3 and ω_3 known, u_1 and u_2 can be obtained by solving simultaneously

$$\frac{\partial u_1}{\partial x_1} + \frac{\partial u_2}{\partial x_2} = -\frac{\partial u_3}{\partial x_3} \tag{6}$$

and

$$\frac{\partial u_2}{\partial x_1} - \frac{\partial u_1}{\partial x_2} = \omega_3. \tag{7}$$

The pressure field is not needed in the calculation but can be obtained whenever necessary.

The boundary conditions are $u_1 = u_2 = u_3 = 0$ (no-slip) on a wall, and $\partial u_1/\partial x_3 = \partial u_2/\partial x_3 = 0$, $u_3 = 0$ at the free surface.

To represent the solutions in space, finite Fourier expansions in the homogeneous (x_1 and x_2) directions are used. In the normal direction x_3, they are represented by Chebyshev polynomials, i.e.

$$f(x_1, x_2, x_3) = \Sigma_{k_1} \Sigma_{k_2} \Sigma_{k_3} \hat{a}(k_1, k_2, n_3) \times e^{(k_1 x_1 + k_2 x_2)} \cdot T_{n_3}(x_3). \tag{8}$$

The wave numbers k_1 and k_2 are given by

$$k_1 = 2\pi n_1 / L_1, \quad k_2 = 2\pi n_2 / L_2 \tag{9}$$

where L_1 and L_2 are the periodicity lengths in the streamwise and spanwise directions, correspondingly. A full description of the numerical scheme can be found in Lam (1989).

The approximate form of the equation for the motion of a particle is:

$$m_p \frac{d\bar{v}}{dt} = \frac{3}{4} C_D \frac{\rho}{\rho_p} \frac{1}{d_P} |\bar{u} - \bar{v}| m_p (\bar{u} - \bar{v}) f(H) + m_f \frac{D\bar{u}}{Dt} + \frac{1}{2} m_f \frac{d}{dt}(\bar{u} - \bar{v}) + (m_p - m_f)\bar{g} + 6\pi \left(\frac{d_p}{2}\right)^2 \mu \int_{t_0}^{t} \frac{d}{d\tau}(\bar{u} - \bar{v}) [\pi \nu (t - \tau)]^{-0.5} d\tau \tag{10}$$

where the drag coefficient is given by White (1991)

$$C_D = \frac{24}{Re_p} + \frac{6}{1 + Re_p^{0.5}} + 0.4, \quad 0 < Re_p < 2 \cdot 10^5 \tag{11}$$

and where Re_p is the particle Reynolds number

$$Re_p = \frac{|\bar{v} - \bar{u}| d_p}{\nu}$$

where m_p is the mass of the particle, μ is the fluid viscosity, $\bar{v}$ is the particle velocity, $f(H)$ is the coefficient of wall effect on the Stokes drag, H is the distance from the center of the particle to the wall, m_f is the mass of the fluid displaced by the particle, $\bar{g}$ is the acceleration due to gravity, d/dt is the time rate of change following the particle, $D\bar{u}/Dt$ is the total acceleration of the fluid as seen by the particle. The coefficient of wall effect is given by Kim and Karrila (1991) for a particle moving parallel to a wall

$$f(H) = \frac{1}{1 - \frac{9}{16}\frac{d_p}{2H} + \frac{1}{8}\left(\frac{d_p}{2H}\right)^3} \tag{12}$$

and for a particle moving perpendicular to a wall

$$f(H) = \frac{1}{1 - \frac{9}{8}\left(\frac{d_p}{2H}\right) + \frac{1}{2}\left(\frac{d_p}{2H}\right)^3} \tag{13}$$

In Eq. [10] it is customary to neglect the Basset term, the last term on the r.h.s. of the equation, in order to conserve computational time.

When the particle is small, in the sense that $Re_p \ll 1$, the effect of the particle on the flow field can be fed back explicitly at every time-step through a point force acting on the fluid. Such small particles are subgrid size, and, therefore, the force has to be distributed to the surrounding mesh points, see Pan and Banerjee (1996). In the case of large particles, which cover many mesh, or collocation, points in the fluid, to get a detailed resolution of the flow pattern around a coarse particle, one needs to consider a very fine distortion of space in the vicinity of the particle, that requires a rather large number of nodes. Because of the computer

memory limitations, we could not get a high resolution in the vicinity of a single particle. In our calculations, particles occupied two nodes in the x_1-direction, and four nodes in the x_2-direction. The number of nodes occupied by a particle in the x_3-direction (normal to the bottom of the channel), depends on the position of the particle in the flow and takes up to 35 nodes near the wall.

The general calculation scheme is:

1. The flow field is brought to a stationary state without particles.
2. Particles are introduced into this flow field, and their motion is calculated with a one-way coupling, i.e. by using Eqs. (10)–(13). The particles are allowed to reach stationary distribution with regards to their position, velocities etc. At this stage, the particles were considered as points. Since the particles are relatively large, each covers a number of collocation points, and is moved about by an implicit scheme. The fluid velocity at the various locations in the particle (which is known from step 1) is averaged with a three-dimensional cubic spline interpolation scheme, and this velocity is then applied on the particle through Eq. (10).
3. Two-way coupling is now introduced. To do that all the velocities in the collocation points occupied by the particle (known from step 1) were made to be equal by using Eq. (2) with an additional source term S_{pi}. This source term is introduced into Eq. (2):

$$\frac{\partial u_i}{\partial t} = S_i + \frac{1}{Re}\nabla^2 u_i - \frac{\partial p}{\partial x_i} - S_{\mathrm{pi}} \tag{14}$$

and this equation is solved until all collocation points in the particle have the same velocity. This required iteration, since one does not know a priori the exact form of the source term S_{pi} which will make the fluid velocity equal to the particle velocity at the collocation points occupied by the particles. In this connection, the iteration process is as following: at time t_n the solution of the flow field (without particles) is u_{in} and the source term is S_{in}. The particle, at this time step, is moving at velocity v_{pn}. Now all collocation points inside the particle are assigned a velocity v_{pn}. Thus, a new flow-field is obtained with velocity $u_{\mathrm{in}}^{(1)}$ everywhere except inside the particles where the velocities are v_{pn}. Numerically, the whole procedure is equivalent to a series of iterations of the Navier–Stokes equations Eqs. (14). The iteration stops at $\tau = N\Delta\tau$ when specified convergence criteria are satisfied. The step for iteration, $\Delta\tau$, is the step which converges the source term to the desired value required to match the boundary conditions on the particle. This step is different from the time step Δt for proceeding with the fluid and particle motion computation. While $\Delta\tau$ is related to the stability and the speed of convergence of the iteration, Δt is determined by the accuracy requirement for calculation of fluid motion, i.e. the smallest time scale, one wants to resolve in fluid flows.

In the present work, the iteration was stable at $\Delta\tau = 0.01\ \Delta t$. Convergence criteria are set such that the relative error of velocities, averaged over all the collocation points inside and on the particle, is less than 0.5%.

Particle velocity is calculated through an implicit scheme. It is necessary to evaluate the instantaneous fluid velocity at the location of the particle accurately. In this connection, a three

dimensional cubic spline interpolation scheme was used. This scheme was applied in the three coordinate directions at the particle location. The new position of the particle was calculated as

$$\bar{x}_p(t_{n+1}) = \bar{x}_p(t_n) + \frac{1}{2}\Delta t[\bar{v}(t_{n+1}) + \bar{v}(t_n)]. \tag{15}$$

In the present study, the turbulent channel flow of Reynolds number $Re^* = 85.4$ is simulated. The $Re^* = 2hu^*/\nu$ is based on shear velocity u^*, and the half depth of the flume. The bulk Reynolds number $Re = 2hU/\nu$ in this case is 2600, where $2h$ is the flow depth, $2h = 37$ mm, U is the mean streamwise velocity. The calculations were carried out for clean water and for particle-laden flow with dimensionless particle diameter $d^+ = 8.5$ and $d^+ = 17$, and concentration $c = 2.6{\cdot}10^{-4}$. The calculations were carried out in a computational domain of $1074 \times 537 \times 171$ wall units in the x_1, the x_2 and the x_3 directions with a resolution of $128 \times 128 \times 129$. A nonuniform distribution of collocation points is used in the wall-normal (x_3) direction due to the nature of the Chebyshev polynomials, and the first collocation point away from the wall is at $x_3^+ = 0.1$. The density of particles was 1050 kg/m^3

3. Results and discussion

3.1. Comparison with experimental data

As a check on the numerical simulation, the data taken from the experiments of Kaftori et al. (1995a, b) are used to compare with numerically calculated values. The simulations were performed for the particle-laden flow with dimensionless particle size $d^+ = 8.5$ and concentration $c = 2.6{\cdot}10^{-4}$. The comparison is shown in Fig. 2 for the streamwise, u_1', velocity

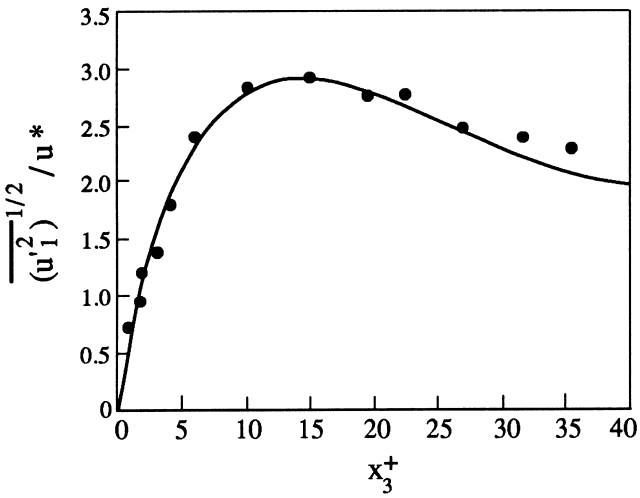

Fig. 2. Comparison of streamwise turbulence intensities of numerical simulation with the experimental data, $d^+ = 8.5$.

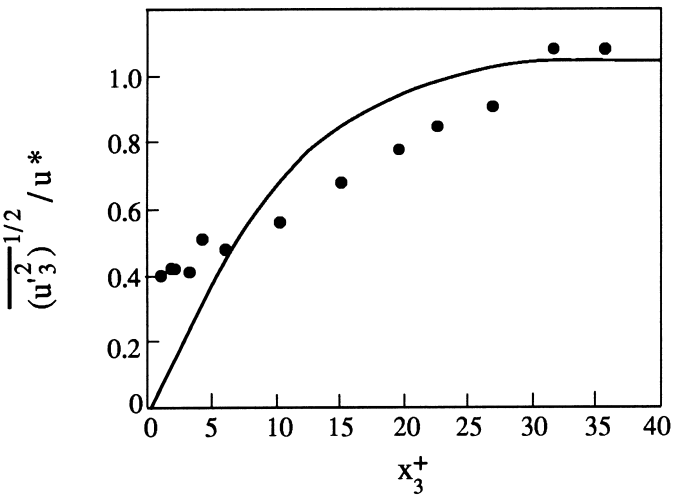

Fig. 3. Comparison of wall-normal turbulence intensities of numerical simulation with the experimental data, $d^+ = 8.5$.

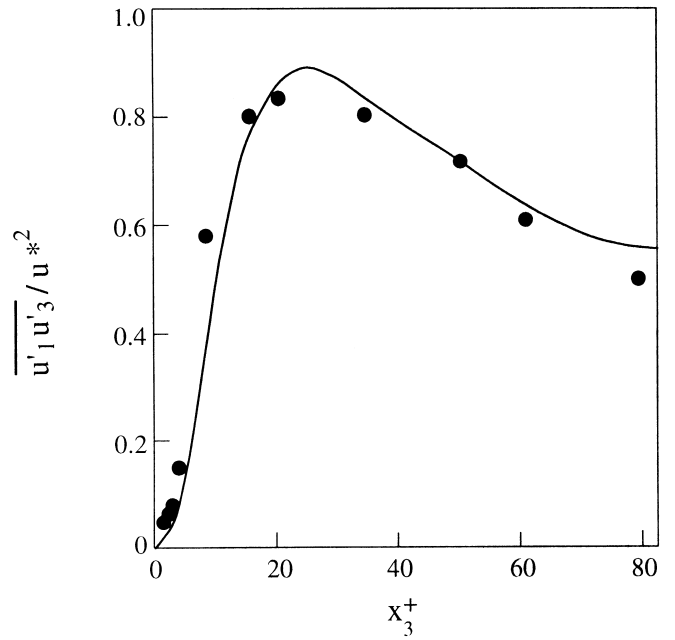

Fig. 4. Comparison of Reynolds stress of numerical simulations with the experimental data, $d^+ = 8.5$.

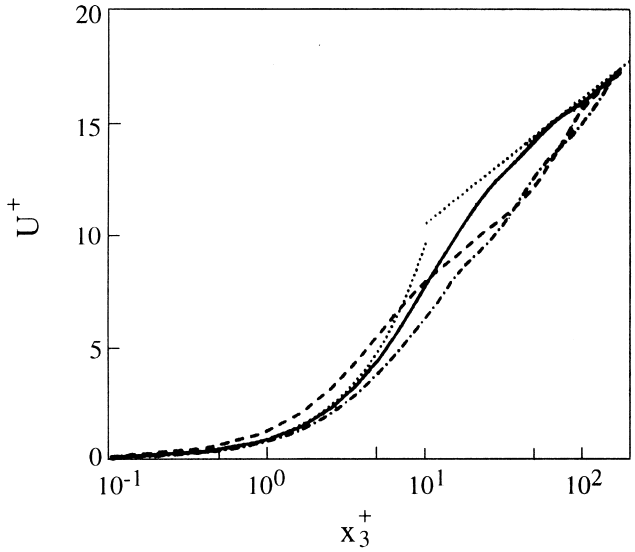

Fig. 5. Mean streamwise velocity in wall variables: —— clean water; –·– $d^+ = 8.5$;— $d^+ = 17$.

fluctuations, in Fig. 3 for the wall normal velocity fluctuations, u_3', and in Fig. 4 for Reynolds stress, $u_1'u_3'$. The solid line represents the DNS results and the points represent the experimental values with the same particle size and concentration. The velocity fluctuations and wall normal coordinate, x_3, are normalized by the wall friction velocity, u^*. The numerical results of u_1' and $u_1'u_3'$ distribution agree quite well with the experimental data, particularly in the near wall region at $x_3^+ \leq 5$. The numerical results of u_3' distribution reach reasonable agreement at $x_3^+ > 5$.

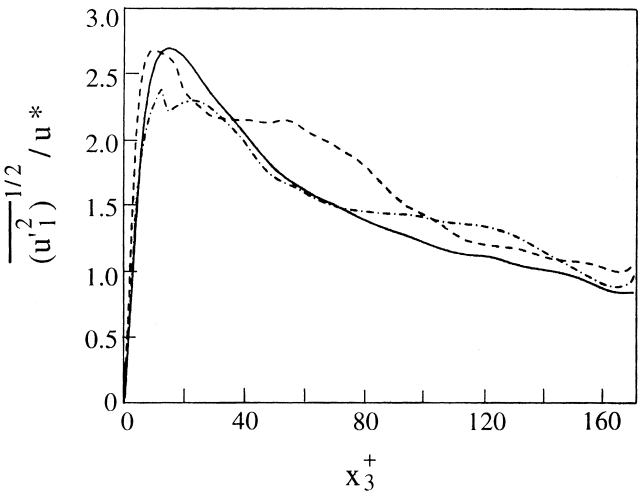

Fig. 6. Dimensionless streamwise velocity fluctuations: —— clean water; –·– $d^+ = 8.5$;— $d^+ = 17$.

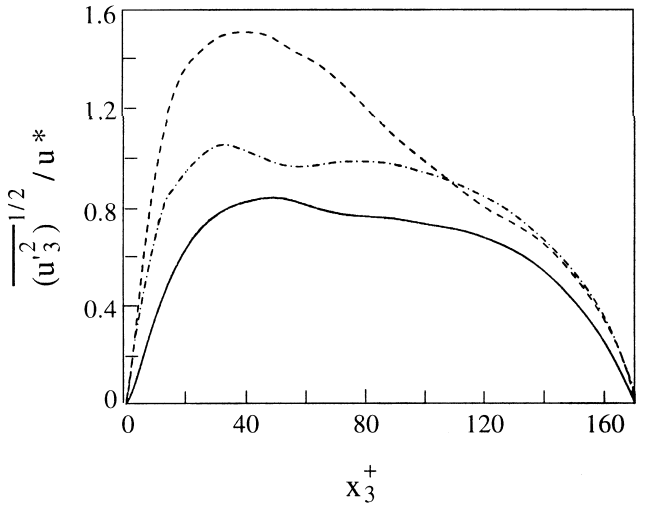

Fig. 7. Dimensionless wall normal velocity fluctuations: —— clean water; –·– $d^+ = 8.5$;— $d^+ = 17$.

3.2. Effect of particle size on the turbulent velocity field

The DNS results are shown in Fig. 5–9 in wall variables, and the results for clean water are presented by a solid line, the results for particle - laden flow are presented by dashed lines. Fig. 5 shows the effect of particles on the mean streamwise velocity. The usual clean flow profiles $U^+ = x_3^+$ $(x_3^+ \leq 10)$ and $U^+ = 2.5\ \ell n\ x_3^+ + 5.0$ $(x_3^+ > 10)$ are also plotted (dotted line) for comparison. For the flow with particles $d^+ = 8.5$ in the region $x_3^+ > 10$ the mean velocity decreases. This effect is similar to the rough wall effects as reported by White (1991). For $d^+ = 17$ particles in the region $x_3^+ < 10$ the mean velocity increases. This is due to the

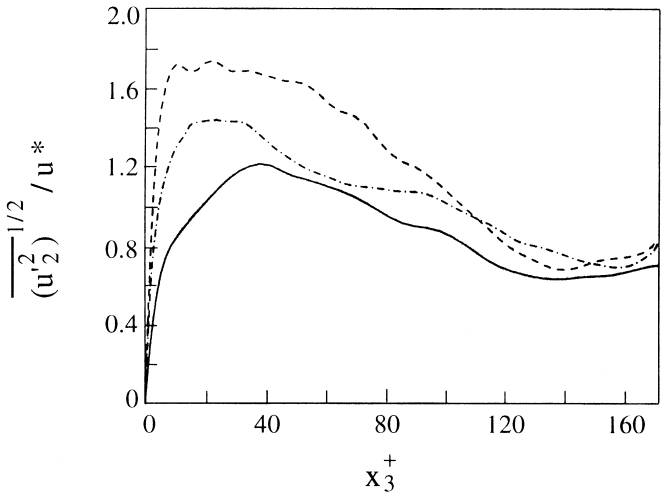

Fig. 8. Dimensionless spanwise velocity fluctuations: —— clean water; –·– $d^+ = 8.5$;— $d^+ = 17$.

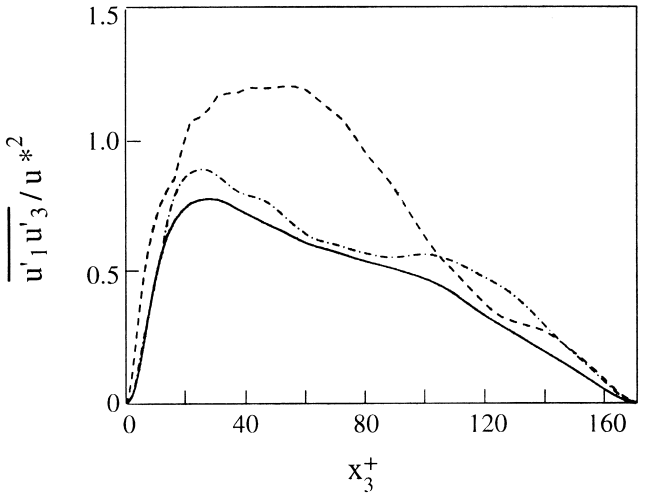

Fig. 9. Dimensionless Reynolds shear stress: —— clean water; –·– $d^+ = 8.5$;— $d^+ = 17$.

fact that the lower part of the particle moves faster than the surrounding fluid. Unlike the case with the particles $d^+ = 8.5$, the particles $d^+ = 17$ do not behave like wall roughness.

Dimensionless streamwise turbulence intensity is shown in Fig. 6. The changes in the streamwise velocity fluctuations seem not significant in the near wall region at $x_3^+ \leq 40$. The small changes in the u_1' indicate that the particles closely follow the fluid motion in the streamwise direction. Unlike this case, the changes in wall normal, Fig. 7, and spanwise velocity fluctuations, Fig. 8, increase when the particle size d^+ increases. The Reynolds shear stress is shown in Fig. 9. The significant enhancement in the Reynolds stress was observed, when the particle size changed from $d^+ = 8.5$ to $d^+ = 17$. The zone of the significant influence of the $d^+ = 17$ particles on Reynolds stress is about $x_3^+ = 100$.

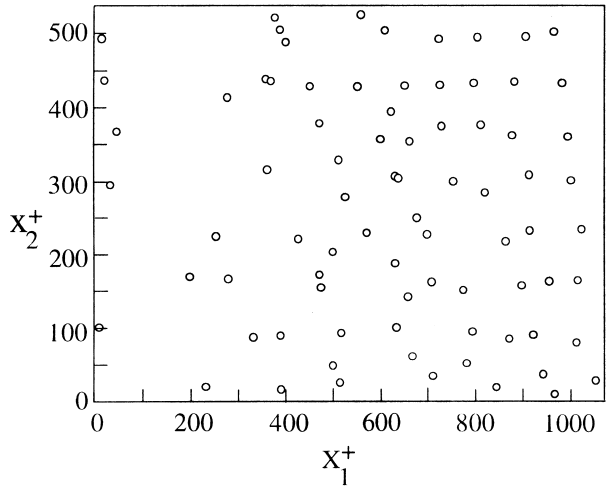

Fig. 10. Distribution of particles in the x_1, x_2 plane. Numerical simulations.

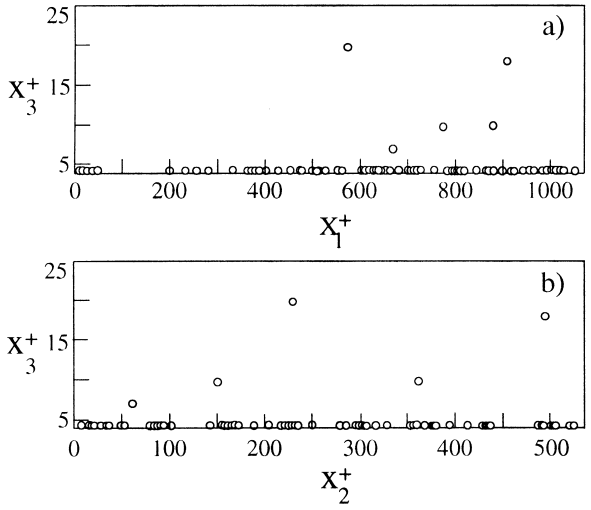

Fig. 11. Distribution of particles in the x_1, x_3 and x_2, x_3 plane. Numerical simulations.

3.3. Particle motion in the boundary layer

Particle size may play an important role in the motion of a particle in turbulent flows. For $d^+ = 8.5$ the particles distribution in x_1, x_2 plane is shown in Fig. 10, and distribution in x_1, x_2 and x_2, x_3 plane is shown in Fig. 11. An interesting result of the present study is that particles are distributed uniformly, i.e. do not tend to segregate in the low speed streaks. This is in complete agreement with our experimental observations. An example of the typical situation observed from plan views of the flow in the flume is shown in Fig. 12. This observation indicates that the tendency of particles to agglomerate into the streaks depends on

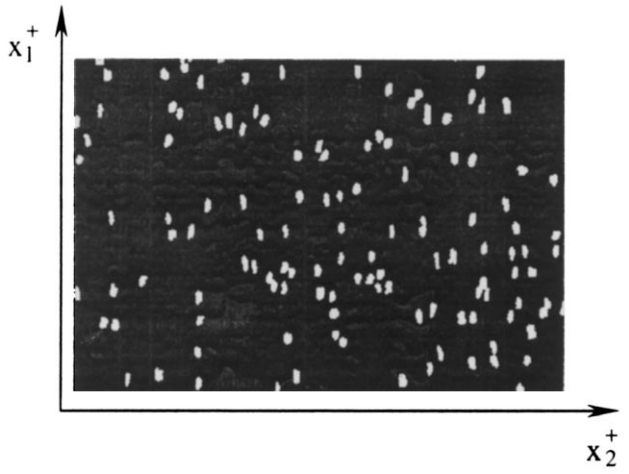

Fig. 12. Distribution of particles in the x_1, x_2 plane. Experimental data.

the particle size and flow conditions. Reviews for particle behaviour in turbulent flow can be found in McCoy and Hanratty (1977) and Papavergos and Hedley (1984), where the experimental and theoretical results are presented. A key parameter is the particle relaxation time which is a dimensionless measure of particle inertia, and reflects how closely particles follow fluid streamlines. Pedinotti et al. (1992) performed a DNS of particle behaviour in the wall region of a turbulent channel flow. They found that maximum sorting is obtained for values of $\tau_p^+ = 3$. For smaller values of τ_p^+ the particles tend to distribute uniformly along the bed, and the same happens for larger values of τ_p^+.

4. Conclusions

This study examines the modulation of turbulence due to the two-way coupling between near-wall region of turbulent fluid and coarse particles. It has been shown that the coarse particles significantly modify the velocity fluctuations of the carrier fluid, and an augmentation of intensity of turbulence and Reynolds stress increases with an increase of particle diameter. It has been demonstrated that the particles with great value of relaxation time do not accumulate along the low-speed streaks.

Acknowledgements

This research was supported by the Basic Research Foundation administered by the Israel Academy of Sciences and Humanities and by the Ministry of Science, State of Israel. The research was also supported by the Fund of the Promotion of Research at the Technion.

References

Banerjee, S., 1994. Direct numerical simulation of multiphase turbulent flows. Russian J. Engng. Thermophys 4, 119–135.

Buyevich, Yu., Gupalo, P., 1965. An influence of suspended particles on a decay of isotropic turbulence in a liquid. J. Prikladnaya Mechanics and Technic. Physica 4, 89–96.

Elghobashi, S., Truesdell, G.C., 1993. On the two-way interaction between homogeneous turbulence and dispersed solid particles. I: Turbulent modification. Phys. Fluids. A5. 1790–801.

Gore, R.A., Crowe, C.T., 1989. Effect of particle size on modulating turbulent intensity. Int. J. Multiphase Flow 15, 279–285.

Hardalupas, Y., Taylor, A.M.K.P., Whitelaw, J.H., 1989. Velocity and particle-flux characteristics of turbulent particle-laden jets. Proc. R. Soc. London A426, 31–78.

Hetsroni, G., Sokolov, M., 1971. Distribution of mass, velocity and intensity of turbulence in two-phase jet. J. Appl. Mech. 38, 315–327.

Hetsroni, G., 1989. Particle-turbulence interaction. Int. J. Multiphase Flow 15, 735–746.

Hetsroni, G., Rozenblit, R., 1994. Heat transfer to a liquid–solid mixture in a flume. Int. J. Multiphase Flow 20, 671–689.

Kaftori, D., Hetsroni, G., Banerjee, S., 1995a. Particle behaviour in the turbulent boundary layer. I. Motion, depositin and entrainment. Phys. Fluids 7, 1095–1106.

Kaftori, D., Hetsroni, G., Banerjee, S., 1995b. Particle behaviour in the turbulent bundary layer. II. Velcoity and distribution profiles. Phys.Fluids 7, 1107–1121.

Kim, S., Karrila, S., 1991. Microhydrodynamics. Butterworth, London.

Lam, K.L., 1989. Numerical investigation of turbulent flow bounded by a wall and a free-slip surface. PhD thesis, University of California, Santa Barbara.

Lam, K.L., Banerjee, S., 1988. Investigation of turbulent flolw bounded by a wall and a free surface. In: E.E. Michaelides, M.P. Sharma (Ed.). Fundmentals of Gas–Liquid Flows, vol. 72. ASME, Washington, DC, pp. 29–38.

Levy, Y., Lockwood, F.C., 1981. Velocity measurements in a particle-laden turbulent free jet. Combustion and Flame 40, 333–339.

McLaughlin, J.B., 1994. Numerical computation of particle-turbulence interaction. Int. J. Multiphase Flow 20, 211–232.

McCoy, D.D., Hanratty, T.J., 1977. Rate of deposition of droplets in annular, two-phase flow. Int. J. Multiphase Flow 3, 319–331.

Nino, Y., Garcia, M.H., 1996. Experiments on particle–turbulence intractions in the near-wall region of an open channel flow: implications for sediment transport. J. Fluid Mech. 326, 285–319.

Pan, Y., Banerjee, S., 1996. Numerical simulation of particle interactions with turbulence. Phys. Fluids 8, 2733–2755.

Pan, Y., Banerjee, S., 1997. Numerical investigation of the effects of large particles on wall-turbulence. Phys. Fluids 9, 3786–3807.

Papavergos, P.G., Hedley, A.B., 1984. Particle deposition behaviour from turbulent flows. Chem Engng. Res. Des. 62, 275–295.

Parthasarathy, R.N., Faeth, G.M., 1987. Structure of a turbulent particle-laden water jet in still water. Int. J. Multiphase Flow 13, 699–714.

Pedinotti, S., Martiotti, G., Banerjee, S., 1992. Direct numerical simulation of particle behaviour in the wall region of turbulent flows in horizontal channels. Int. J. Multiphase Flow 18, 927–941.

Tsuji, Y., Morikawa, Y., Tanaka, T., Kazimine, K., Nishida, S., 1988. Measurements of an axisymmetric jet laden with coarse particles. Int. J. Multiphase Flow 14, 566–574.

Vinberg, A.A., Zaichick, L.I., Pershukov, V.A., 1991. Computational model for turbulent gas-particle jet streams. J. Engng. Phys. 61, 554–563.

White, F.M., 1991. Viscous Fluid Flow. McGraw-Hill, New York.

Yarin, L.P., Hetsroni, G., 1993. Turbulence intensity in dilute two-phase flow-3. Int. J. Multiphase Flow 20, 27–44.